P H Y S I C A L   R E V I E W   L E T T E R S

Dynamic Colloidal Stabilization by Nanoparticle Halos

S. Karanikas and A. A. Louis*

Department of Chemistry, Cambridge University, Lensfield Road, Cambridge CB2 1EW, United Kingdom
(Received 22 September 2004; published 7 December 2004)

We explore the conditions under which colloids can be stabilized by the addition of smaller particles. The largest repulsive barriers between colloids occur when the added particles repel each other with soft interactions, leading to an accumulation near the colloid surfaces. At lower densities these layers of mobile particles (nanoparticle halos) result in stabilization, but when too many are added, the interactions become attractive again. We systematically study these effects—accumulation repulsion, reentrant attraction, and bridging—by accurate integral equation techniques.

Colloidal dispersions—solid particles with radii ranging from a few nm to a few μm, suspended in a liquid solvent—are common in nature and widely used in industry. Blood, paint, ink, and cement are typical examples. Because interatomic dispersion forces induce effective van der Waals interactions with large attractive values at contact, colloids will irreversibly aggregate, which is usually undesirable, unless their surfaces are prevented from approaching too closely. The two most common ways to achieve this are called *steric* and *charge stabilization* [1]. Popular strategies for steric stabilization usually involve grafting a layer of polymers onto the colloid surface, resulting in dense repulsive brushes that prevent close contact. For charge stabilization, the route most common in nature, the colloids have surface charges of the same sign, leading to a double layer of microscopic coions and counterions. Adding this effective repulsion to the intrinsic van der Waals attraction results in the famous Derjaguin-Landau-Verwey-Overbeek potential [2], with a metastable free-energy barrier preventing aggregation.

In an important recent development, a third strategy for colloidal stabilization, termed *nanoparticle haloing*, was introduced by Tohver and co-workers [3]. By adding charged hydrous zirconia nanoparticles of average radius 3 nm to a suspension of (marginally charged) colloidal silica spheres of radius 285 nm in deionized water, the following behavior was observed: For low nanoparticle concentrations the silica spheres aggregate, driven by the generic van der Waals attractions. At intermediate nanoparticle concentrations, the dispersion becomes stable, whereas at higher concentrations the silica spheres aggregate again. The authors [3] attribute the initial stabilization to layering of the small nanoparticles near the colloidal surfaces. These "halos" occur because it is advantageous for the charged nanoparticles to be near the uncharged colloid surfaces. When two colloids then approach each other, their respective halos repel, preventing aggregation. The reentrant aggregated phase, observed at higher nanoparticle concentrations, was attributed to normal entropic depletion attraction [4].

Clearly, a new route to stabilize colloids would have many potential applications. Indeed, nanoparticle haloing has already been used to enhance the self-assembly of 3D colloidal crystals on patterned surfaces [5]. Nevertheless, even though this novel stabilization strategy has been demonstrated by experiment, many questions remain about its generic applicability. To address these issues we carry out a systematic theoretical study of the effective interaction $\beta V_{bb}^{\mathrm{eff}}(r)$ [6] between colloids, induced by (much) smaller particles ($\beta^{-1} = k_B T$ is the reduced temperature). We find a large regime of parameter space where $\beta V_{bb}^{\mathrm{eff}}(r)$ is repulsive enough for stabilization, but this is usually followed by reentrant attraction at a higher small particle packing fraction. The picture that emerges is considerably more subtle than that of a static layer of adsorbed particles akin to steric stabilization. Instead, the nanoparticle halos are dilute, and in dynamic equilibrium with the bulk solution. Moreover, we observe no obvious change in their character when the reentrant attraction kicks in, implying that this phenomenon is more complex than simple depletion attraction.

The key quantity we study is $\beta V_{bb}^{\mathrm{eff}}(r)$, the effective interaction between two spheres of diameter σ_{bb}, induced by smaller spheres. Its properties are determined by the number density $\rho_s = N_s/V$ of small particles and by the interactions $\beta\Phi_{bs}(r)$ and $\beta\Phi_{ss}(r)$; it is independent of the intrinsic interaction $\beta\Phi_{bb}(r)$ [7]. Introducing small particles that induce a $\beta V_{bb}^{\mathrm{eff}}(r)$ repulsive enough to counteract an attractive $\beta\Phi_{bb}(r)$ will stabilize the colloids.

The basic big-small and small-small interactions $\beta\Phi_{ij}(r)$ are modeled by a hard-core Yukawa form which is versatile without having too many parameters to vary [7]. $\beta\Phi_{ij}(r) = \infty$ if $r < \sigma_{ij}$; $\beta\Phi_{ij}(r) = \phi_{ij}(r)$ for $r > \sigma_{ij}$, where in each case r denotes the distance between the centers of the particles, and the Yukawa tail is

$$\beta\phi_{ij}(r) = \frac{\beta\epsilon_{ij}\sigma_{ij}}{r}\exp\left[-\frac{(r-\sigma_{ij})}{\lambda_{ij}}\right], \qquad (1)$$

where $\sigma_{bs} = \frac{1}{2}(\sigma_{bb} + \sigma_{ss})$ with σ_{ss} the small particle

hard-core diameter. By varying the size ratio $q = \sigma_{ss}/\sigma_{bs}$, packing fraction $\eta_s = \frac{1}{6}\pi\rho_s\sigma_{ss}^3$, and the four dimensionless potential parameters $\beta\epsilon_{ss}$, $\beta\epsilon_{bs}$, λ_{ss}/σ_{ss}, and λ_{bs}/σ_{bs}, a wide variety of different physical situations can be studied [7]. For repulsive interactions, for example, Eq. (1) is a good model for charged suspensions [8].

To restrict this vast parameter space somewhat, and inspired by the successful experiments [3], we choose $\epsilon_{ss} > 0$ and, initially, $\epsilon_{bs} = 0$. The effective potentials $\beta V_{bb}^{\text{eff}}(r)$ are calculated by using the two-component Ornstein-Zernike (OZ) equations in the $\rho_b \rightarrow 0$ limit where they decouple, together with the hypernetted chain (HNC) integral equation closure [9], leading to $\beta V_{bb}^{\text{eff}}(r) = -\rho_s \int d\mathbf{r}' h_{bs}(r)c_{bs}(|\mathbf{r}' - \mathbf{r}|)$, where $h_{bs}(r) = g_{bs}(r) - 1$ with $g_{bs}(r)$ the pair correlation function between big and small particles, and $c_{bs}(r)$ is the direct correlation function [9]. In this limit, HNC has some important advantages [10] over other popular integral equations such as Percus-Yevick (PY) or Rogers-Young [9]. For example, it is exact for the Asakura-Oosawa (AO) model [4] at all densities ρ_s (PY is not [10,11]). Moreover, HNC is known to be particularly accurate for soft repulsive potentials of the type we are investigating [9]. To validate our method, we compare, in Fig. 1, the performance of HNC with several simulations [7] for $\epsilon_{ss} > 0$ and find excellent agreement. Since we also want to study rather extreme size ratios, we compare, in Fig. 1(b), to depletion potentials for hard spheres (HS) calculated with an accurate density functional theory (DFT) approach [12]. Again HNC performs remarkably well. These results provide the confidence that, even if HNC is not perfectly quantitative, the trends we uncover will be robust, provided we limit ourselves to soft repulsions and low packing fractions [13]. Fortuitously, this appears to be the regime where the nanoparticle haloing mechanism operates most effectively.

In order to systematically investigate the conditions for which repulsive stabilization occurs, we calculated, with HNC, $\beta V_{bb}^{\text{eff}}(r)$ for a large number of parameter combinations. Two typical examples are shown in Fig. 2, demonstrating the common pattern we find: for increasing packing fractions a maximum first appears close to contact and continues to increase until at higher η_s a secondary minimum appears that grows with η_s and rapidly moves to a separation of about one σ_{ss}. This sequence of initial stabilization followed by reentrant attraction is similar to that seen in the experiments [3] and is found throughout the parameter regime we investigated.

To further quantify the region of stability, we choose the following measure: For a given set $\beta\epsilon_{ss}$, λ_{ss}/σ_{ss}, and q, we calculate the effective potentials for different η_s, as done for Fig. 2. The "stability window" is defined as $\Delta_\eta = \eta_s^u/\eta_s^s$, where η_s^s is the packing fraction above which the maximum of $\beta V_{bb}^{\text{eff}}(r)$ is >5 (leading to kinetic stabilization), and η_s^u is the packing fraction below which the minimum of $\beta V_{bb}^{\text{eff}}(r)$ is < -2 (a conservative esti-
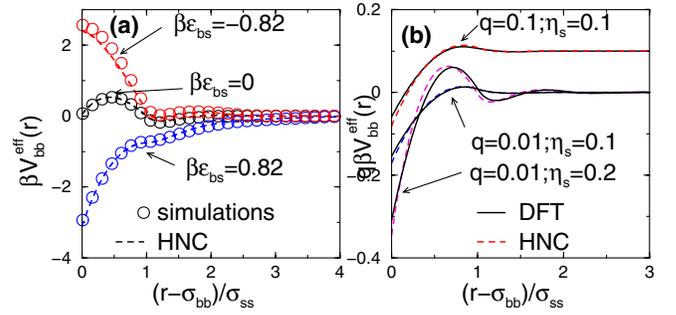
FIG. 1 (color online). (a) Comparison of simulations (from [7]) and HNC calculations of the effective potential $\beta V_{bb}^{\text{eff}}(r)$. The size ratio $q = 0.2$, and the potential parameters $\lambda_{ss}/\sigma_{ss} = 1/3$, $\lambda_{bs}/\sigma_{bs} = 1/1.2$, and $\beta\epsilon_{ss} = 2.99$ are kept constant, while $\beta\epsilon_{bs}$ is varied. (b) HNC and DFT [12] calculations for small size ratios q. To facilitate comparisons, we plot $q\beta V_{bs}^{\text{eff}}(r)$ and shift the curve for $q = 0.1$ up by $+0.1$.

mate of where short-range attractions induce aggregation [11]). The way our stability measure Δ_η varies with potential parameters is depicted in Fig. 3, from which some general trends can be extracted: The size of the window increases with increasing λ_{ss}/σ_{ss} and decreasing $\beta\epsilon_{ss}$ and q. [In the HS limit ($\beta\epsilon_{ss} = 0$) we find no window of stability.] For a number of points (A–D) in Fig. 3, we show the values of η_s^u and η_s^u. As expected, these packing fractions decrease with increasing $\beta\epsilon_{ss}$ and λ_{ss}/σ_{ss} since the small particles repel each other more and have a larger effective "size."

The effective repulsion is clearly related to the accumulation of particles near the colloids (nanoparticle halos [3]). We define the "halo" as those particles between $r = \sigma_{bs}$ and $r = r_{\min}$, the distance at which the pair correlation function $g_{bs}(r)$ has its first minimum. The number of particles N_{halo} follows from integrating $g_{bs}(r)$ up to $r_{\min}$. The 2D packing fraction is given by $\eta^{2D} = \frac{1}{4}\pi\rho^{2D}\sigma_{ss}^2$, where $\rho^{2D} = N_{\text{halo}}/(4\pi\sigma_{bs}^2)$. For all the parameters studied we find the same behavior depicted in the inset of Fig. 3: The halo packing fraction η^{2D} is linear with η_s, and there is no change of slope or other obvious property
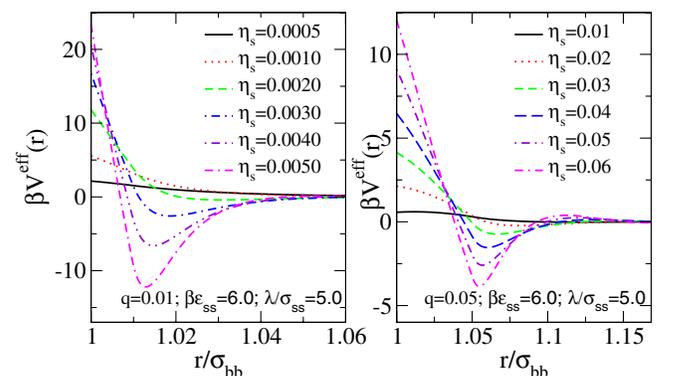
FIG. 2 (color online). Two typical examples of the effective potentials. First there is initial stabilization, and then a reentrant attraction.
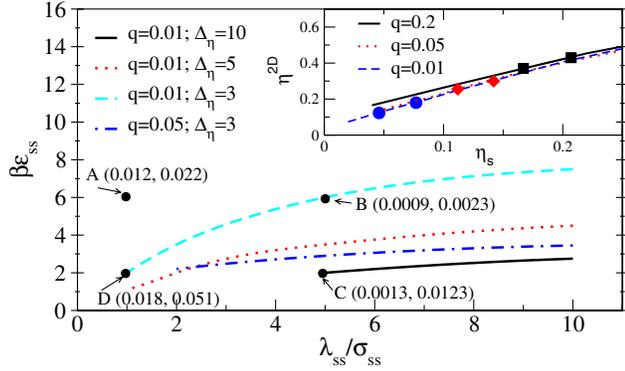
FIG. 3 (color online). The "equi-Δ_η" lines denote different values of the stability window $\Delta_\eta = \eta_s^u/\eta_s^s$ for size ratios $q = 0.01$ and $q = 0.05$. For points A–D the stability window packing fractions, for $q = 0.01$, are listed in the format (η_s^s, η_s^u). Inset: the 2D packing fraction η^{2D} of a halo for different size ratios q. The potential parameters are $\beta\epsilon_{ss} = 2$ and $\lambda_{ss}/\sigma_{ss} = 0.5$. The symbols denote η_s^s and η_s^u for $q = 0.01$ (circles), $q = 0.05$ (diamonds), and $q = 0.1$ (squares).

marking either the beginning of stabilization at η_s^s or reentrant attraction at η_s^u. We have also investigated other surface properties such as the adsorption $\Gamma_s = -\int h_{bs}(r)d\mathbf{r}$ and the related surface tension γ_s [14]. In contrast to polymeric depletants, where γ_s helps determine $\beta V_{bb}^{\text{eff}}(r)$ [14], we observe no clear signatures of η_s^s or η_s^u in the surface tension or the adsorption.

For small q we expect the $g_{bs}(r)$ to be similar within corrections $\mathcal{O}(q^{-1})$, which explains why the η^{2D} vs η_s curves are so close for different q. However, the stability windows, shown by the symbols in the inset of Fig. 3, differ significantly: They are at lower η_s for smaller q, something we observe more generally. This can be understood from an approximate Derjaguin [1] argument valid in the small q limit. The potentials scale as $1/q$ times the force between two plates, and so stabilization (and reentrant attraction) is achieved at lower packing fractions. However, this does not easily explain why the window size also grows with decreasing q.

The halos are very dilute at stabilization, and we have checked that all layer densities studied are well below that of any two-dimensional freezing transition. In fact, the layers shown in the inset of Fig. 3 are among the densest we investigated; for some Φ_{ss}, η_s^{2D} can easily be an order of magnitude lower at η_s^s. At these low packing fractions, the particles rapidly diffuse between halos and the bulk. In contrast to a steric stabilization mechanism, where the layers are *static*, we emphasize that this nanoparticle halo stabilization mechanism is *dynamic*.

Further evidence against a naive picture of static layers comes from the reentrant attraction. If the halos would become saturated, so that additional small particles can no longer segregate to the colloidal surface and instead act as depletants, then one might expect a linear dependence of the minimum of $\beta V_{bb}^{\text{eff}}(r)$ on η_s as in AO [4] or HS [12] depletion. Instead, the minimum in $\beta V_{bb}(r)$

grows initially as η_s^2, closely resembling the behavior of the second minimum of HS systems [12], which suggests that it has a similar more complex origin in correlation effects. In fact, both minima would be directly related if the potentials were interpreted in terms of a nonadditive HS reference system with $\sigma_{bs} < \frac{1}{2}(\sigma_{bb} + \sigma_{ss})$, as explained in [15]. The repulsive effective interactions found in many other theoretical studies of $\beta V_{bb}^{\text{eff}}(r)$ can also be qualitatively interpreted in this way (see, e.g., [7] and references therein for a discussion), suggesting that nonadditivity may be fruitfully used to interpret the reentrant attraction [10].

One might argue that since adding an attractive $\phi_{bs}(r)$ should increase the number of particles in a layer, this should enhance the stabilization effect. However, we find more subtle scenarios. If we choose $\lambda_{bs} = \lambda_{ss}$, to model residual charge on the large colloids, then for weak attractions the window indeed grows slightly. But, as $\beta\epsilon_{bs}$ becomes more negative, the potentials rapidly develop a large attractive component. This phenomenon, sometimes called *bridging* for polymeric additives [1], results from configurations where the two bigger colloids are both attracted to the same set of smaller particles [10]. An example of bridging is demonstrated in Fig. 4(a) and is representative of what we find more generally: the stability window Δ_η initially grows slightly, but then rapidly disappears, typically around $\beta\epsilon_{bs} \lesssim -1.5$.

On the other hand, a dramatic enhancement of the stabilization occurs for longer ranged colloid-nanoparticle attractions, as demonstrated in Fig. 4 for $\lambda_{bs} = 3\lambda_{ss}$. The bridging effect is bypassed and the first minimum shifts up to positive absolute values; in fact, for these parameters we find no reentrant attraction within the range where we trust HNC [13]. In general, we find this effect for $\lambda_{bs} > \lambda_{ss}$, but exactly where it kicks in depends on q and the other potential parameters. In all cases studied, the 2D layer densities are still very low so that the halos are dilute; typically for more negative $\beta\epsilon_{bs}$ bridging sets in
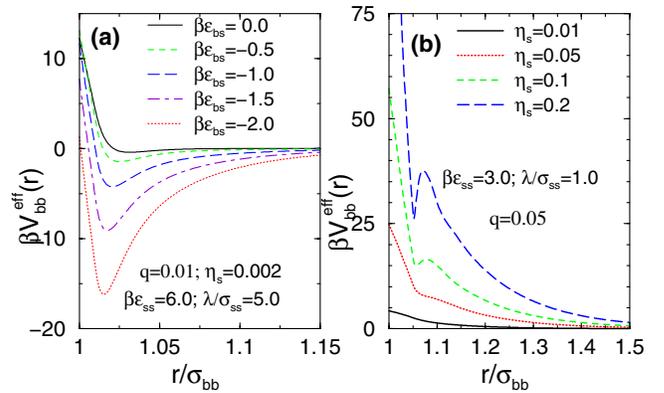
FIG. 4 (color online). (a) Adding an attractive $\beta\phi_{bs}(r)$ generates a deep minimum due to bridging effects when $\lambda_{bs} = \lambda_{ss}$. (b) A dramatic stabilization effect occurs for weak longer ranged attractions: $\lambda_{bs} = 3\lambda_{ss} = 3\sigma_{ss}$, and $\beta\epsilon_{bs} = -0.5$.

again [10]. Of course when $\beta\phi_{bs}(r)$ is attractive enough to induce static saturated layers, then the particles would be sterically stabilized. But technically this is a nonequilibrium effect: it works only if the colloidal particles are first isolated from each other on the time scale that the (saturated) layer forms.

Finally, having systematically explored the effect of different parameters on $\beta V_{bb}^{\mathrm{eff}}(r)$, we make some recommendations for experiments. For $\epsilon_{bs} = 0$ the best stabilization should occur for modestly charged small additives (nanoparticles) since the stability windows are largest for small q, modest $\beta\epsilon_{ss}$, and large λ_{ss}/σ_{ss}. Small σ_{ss} are needed to enhance the latter parameter, since the (Debye) screening length is typically fixed by solution conditions, e.g., $\lambda_{ss} \approx 30$ nm for 0.1 mM monovalent salt concentration. Another argument in favor of small particles concerns the *dynamic* nature of the layers. If the big particles are driven at velocities such that the smaller particles can no longer adiabatically follow, then the stabilization effect may disappear. Since the self-diffusion coefficients of the nanoparticles scale as $1/\sigma_{ss}$ [1], this again favors small particles. Moreover, larger windows Δ_η also enhance stability under halo fluctuations.

Whereas adding charge to the colloids can destroy the stabilization effect, a modest but longer ranged attraction $\beta\phi_{bs}(r)$ can significantly enhance it. The latter effect could be induced by residual van der Waals attractions, although this recommendation must be tempered by the difficulty of adding van der Waals attractions between different species without simultaneously significantly increasing them between similar species. On the other hand, the advantage of small van der Waals attractions (which are independent of debye screening length), is that the ratio $\lambda_{bs}/\lambda_{ss}$ can be tuned by changing salt concentration. This adds another handle for engineering effective potentials and concomitant phase behavior [10].

We observe the same general trends seen in the experiments of Ref. [3], such as lower η_s^s with smaller q and values of η^{2D} well below saturation. A direct quantitative comparison, however, is hampered by their use of polydisperse small particles, and the difficulty in deriving accurate potentials $\beta\phi_{ij}(r)$. Taking their estimates ($\beta\epsilon_{ss} \approx 6$, $\lambda_{ss}/\sigma_{ss} \approx 0.6$) we find a smaller window $\Delta_\eta \approx 2$, at higher η_s than what they observed. The difference could stem from a small attractive $\beta\phi_{bs}(r)$ or from polydispersity (preliminary calculations suggest that this lowers the effective η_s^s and η_s^u [16]).

In conclusion, we discovered a substantial parameter regime where the addition of small (nano) particles can stabilize bigger colloids. Fortuitously, this occurs where the flexible HNC integral equation is most reliable. We usually find a stability window of packing fractions, above or below which the colloids aggregate again. The effects are significantly enhanced for weak longer ranged attractive $\beta\phi_{bs}(r)$. Although the stabilization is clearly related to the formation of diffusive accumulation layers around the bigger particles, we find no simple relationship to layer properties. This suggests these effects are related to more complex correlations. Colloidal stabilization by dynamic nanoparticle halos should be widely applicable and complimentary to existing steric and charge stabilization techniques [1,2]. This new mechanism may also be relevant for smaller scale biological interactions [17].

Note added.—Upon completion of this work we became aware of a study by Liu and Luijten [18] which uses different techniques but arrives at similar conclusions.

*Corresponding author.
Electronic address: aal20@cam.ac.uk

[1] R. J. Hunter, *Foundations of Colloid Science* (Oxford University Press, Oxford, 2001).

[2] E. J. Verwey and J. Th. G. Overbeek, *Theory of the Stability of Lyophobic Colloids* (Elsevier, Amsterdam, 1948).

[3] V. Tohver *et al.*, Proc. Natl. Acad. Sci. U.S.A. **98**, 8950 (2001); V. Tohver, A. Chan, O. Sakurada, and J. A. Lewis, Langmuir **17**, 8414 (2001).

[4] S. Asakura and F. Oosawa, J. Polym. Sci. **33**, 183 (1958); A. Vrij, Pure Appl. Chem. **48**, 471 (1976).

[5] W. Lee *et al.*, Langmuir **20**, 5262 (2004).

[6] C. N. Likos, Phys. Rep. **348**, 267 (2001).

[7] A. A. Louis, E. Allahyarov, H. Löwen, and R. Roth, Phys. Rev. E **65**, 061407 (2002).

[8] J.-P. Hansen and H. Löwen, Annu. Rev. Phys. Chem. **51**, 209 (2000).

[9] J. P. Hansen and I. R. McDonald, *Theory of Simple Liquids* (Academic Press, London, 1986), 2nd ed.

[10] S. Karanikas and A. A. Louis (to be published).

[11] A. A. Louis, Philos. Trans. R. Soc. London A **359**, 939 (2001).

[12] R. Roth, R. Evans, and S. Dietrich, Phys. Rev. E **62**, 5360 (2000). Direct simulations of $V_{bb}^{\mathrm{eff}}(r)$ have only recently become possible for these extreme size ratios: J. Liu and E. Luijten, Phys. Rev. Lett. **92**, 035504 (2004).

[13] No claim is being made for the general accuracy of HNC for all parameter values. For example, the predictions for HS begin to show important quantitative deviations for $\eta_s > 0.3$ and the comparison with simulations of Ref. [7] is less accurate for attractions ($\epsilon_{ss} < 0$).

[14] A. A. Louis, P. G. Bolhuis, E. J. Meijer, and J.-P. Hansen, J. Chem. Phys. **117**, 1893 (2002).

[15] A. A. Louis and R. Roth, J. Phys. Condens. Matter **33**, L777 (2001); R. Roth, R. Evans, and A. A. Louis, Phys. Rev. E **64**, 051202 (2001).

[16] P. Bryk (private communication).

[17] D. Leckband and J. Israelachvili, Q. Rev. Biophys. **34**, 105 (2001).

[18] J. Liu and E. Luijten, Phys. Rev. Lett. **93**, 247802 (2004).